Thermal effects in rotating labyrinth seals

E. Saber and H. A. El-Gamal
Mechanical and Marine Eng. Dept., Arab Academy for Science, Technology and Maritime Transport, Alexandria, Egypt

Modern centrifugal pumps are required to operate at higher pressures and speeds. This requires careful examination of the various design parameters affecting the seal performance. Among these, are the complex geometric parameters along with thermal effects. The unavoidable temperature rise in the seal section is of importance as far as the leakage characteristic is concerned. This has led the authors to examine the effect of the temperature gradients on the performance of the seal. In this paper a thermo-hydrodynamic mathematical model of an axisymmetric labyrinth seal of different geometrical configurations and flow conditions is considered. A (CFD) code is written for the seal design which was developed to permit a rapid and comprehensive calculation of the leakage characteristics for various design parameters. Results were obtained for several case studies and they all showed that the variation of heat flow at inlet clearance is affected considerably by the product of Prandtl number and Eckert number P.E. At small values of P.E the heat is rejected at inlet clearance as long as the aspect ratio is approximately less than 0.6. For a given aspect ratio, increasing P.E increases the generation of heat due to friction and the wormer clearance becomes heated instead of being cooled. The aspect ratio defined here as the critical aspect ratio depending on the temperature difference between the inlet and exit clearances and P.E.

يراد من مضخات الطرد المركزي الحديثة أن تعمل بضغوط وسرعات عالية. ويتطلب ذلك توخي الدقة في فحص العوامل المختلفة الخاصة بالتصميم والتي تؤثر علي أداء موانع التسرب. من بين تلك العوامل توجد عوامل الشكل الهندسي المعقدة مضافا إليها ما هو موجود من تأثيرات حرارية. إن الارتفاع في درجة الحرارة والذي يتعذر تجنبه داخل مانع التسرب له أهمية كبيرة من ناحية خصائص التسرب. هذا ما دفع الباحثين إلي فحص تأثير التدرجات الحرارية علي أداء المانع. حيث تم في هذا البحث دراسة نموذج رياضي هيدروديناميي–حراري لمانع تسرب متماثل محوريا له أشكال هندسية متعددة وظروف تشغيل مختلفة. كما تم عمل برمجية للحاسب تطبق تحليلا عدديا لديناميكا الموائع بغرض عمل الحسابات الخاصة بالمانع للتوصل إلي خصائصه بصورة سريعة وشاملة لمختلف عوامل التصميم. ولقد تم التوصل إلي نتائج لحالات بعينها بينت كلها أن التغير في سريان الحرارة خلال مدخل خلوص المانع يتأثر كثيرا بحاصل ضرب رقم براندتيل في رقم أكيرت P.E . فللقيم الصغيرة لحاصل الضرب تطرد كمية الحرارة من جهة خلوص مدخل المانع طالما أن نسبة الشكل أقل من 0.6 . ولقيمة ما لهذه النسبة فإن زيادة حاصل الضرب هذا يزيد من كمية الحرارة المتولدة نتيجة الاحتكاك ليتم تسخين الخلوص الأعلى في درجة الحرارة بدلا من تبريده. وتعرف نسبة الشكل هنا أنها نسبة الشكل الحرجة والتي تعتمد علي فرق درجة الحرارة ما بين خلوص مدخل وخلوص مخرج مانع التسرب وكذلك علي حاصل الضرب P.E .

Keywords: Labyrinth seals, Non-contact seals, Leakage in turbomachinery, Rotodynamic pump seals, Centrifugal pump seals

1. Introduction

Labyrinth seals have numerous applications that require leakage minimization. The advantages of labyrinth seals are primarily their simplicity and reliability besides their adaptability to radial shaft misalignment occurring in many rotating fluid machinery. In addition they are well suited to a wide range of speeds, temperature and pressure differences. The problem of leakage rate reduction through labyrinth seals, however, has attracted many researchers. Many of the early theoretical treatments to the problem were found to provide results with discrepancies and contradictions [1]. Somewhat reliable predications for the flow through these types of seals were given in [2-4]. For the laminar case the pressure drop leakage rate relationship and the dynamic characteristics of different seal geometries were predicted [5-6]. A theoretical model for a labyrinth seal of arbitrary shape was analyzed assuming that the transverse pressure gradient in the seal is negligible compared to the axial pressure gradient and the seal size small in comparison to shaft radius [7]. On the other hand theoretical and experimental investigation on leakage and dynamic characteristics of stepped labyrinth seals were carried out in an attempt to optimize seal configuration which combines good sealing and satisfactory dynamic performance [8]. In an attempt to improve the prediction accuracy of the performance and dynamic characteristics of the seal, a CFD technique for solving the averaged momentum equations, was carried out in [9]. It is to be noted in this respect that [9] and several previous authors developed their works assuming non-isothermal conditions to take place in the labyrinth cavity and paid no attention to the dependence of fluid viscosity on the temperature gradients inside the seal. The conduction and dissipation of heat inside the seal are of importance no doubt and they seem to contribute mush to the mechanism which drives the leakage flow in the seal cavity especially when the cavity height to shaft radius ratio is small. It is the aim of the present work to consider this effect on labyrinth seal performance.

2. Analysis

The labyrinth seal geometrical configuration and the system of coordinates are shown in fig. 1. The equations governing the incompressible laminar flow of variable viscosity may be written in cylindrical polar coordinates as:

$$\rho\left(v\frac{\partial v}{\partial r}+w\frac{\partial v}{\partial z}-\frac{u^2}{r}\right)=-\frac{\partial p}{\partial r}+2\frac{\partial}{\partial r}\left(\mu\frac{\partial v}{\partial r}\right)+\frac{\partial}{\partial z}\left(\mu\left(\frac{\partial v}{\partial z}+\frac{\partial w}{\partial r}\right)\right)+\frac{2\mu}{r}\left(\frac{\partial v}{\partial r}-\frac{v}{r}\right), \quad (1)$$

$$\rho\left(v\frac{\partial u}{\partial r}+w\frac{\partial u}{\partial z}+\frac{vu}{r}\right)=\frac{\partial}{\partial z}\left(\mu\frac{\partial u}{\partial z}\right)+\frac{\partial}{\partial r}\left(\mu\left(\frac{\partial u}{\partial r}-\frac{u}{r}\right)\right)+\frac{2\mu}{r}\left(\frac{\partial u}{\partial r}-\frac{u}{r}\right). \quad (2)$$

$$\rho\left(v\frac{\partial w}{\partial r}+w\frac{\partial w}{\partial z}\right)=-\frac{\partial p}{\partial z}+2\frac{\partial}{\partial z}\left(\mu\frac{\partial w}{\partial z}\right)+\frac{1}{r}\frac{\partial}{\partial r}\left(\mu r\left(\frac{\partial v}{\partial z}+\frac{\partial w}{\partial r}\right)\right). \quad (3)$$

And the continuity equation is,

$$\frac{\partial v}{\partial r}+\frac{v}{r}+\frac{\partial w}{\partial z}=0 \ . \quad (4)$$

For the above equations it is assumed that the flow is axisymmetric and swirling conditions do not exist. A transformation of the coordinate system is to be performed by letting $r=y+R$ and substituting into eqs. (1-3 and 4) assuming that $R \gg y_{\max}$ (see fig. 1).

$$\rho\left(v\frac{\partial v}{\partial y}+w\frac{\partial v}{\partial z}-\frac{u^2}{R}\right)=-\frac{\partial p}{\partial y}+\mu\left(\frac{\partial^2 v}{\partial y^2}+\frac{\partial^2 v}{\partial z^2}+\frac{1}{R}\frac{\partial v}{\partial y}-\frac{v}{R^2}\right)+2\frac{\partial \mu}{\partial y}\frac{\partial v}{\partial y}+\frac{\partial \mu}{\partial z}\left(\frac{\partial v}{\partial z}+\frac{\partial w}{\partial y}\right), \quad (5)$$

$$\rho\left(v\frac{\partial u}{\partial y}+w\frac{\partial u}{\partial z}+\frac{vu}{R}\right)=\frac{\partial}{\partial z}\left(\mu\frac{\partial u}{\partial z}\right)+\frac{\partial}{\partial y}\left(\mu\left(\frac{\partial u}{\partial y}-\frac{u}{y}\right)\right)+\frac{2\mu}{R}\left(\frac{\partial u}{\partial y}-\frac{u}{R}\right). \quad (6)$$

$$\rho\left(v\frac{\partial w}{\partial y}+w\frac{\partial w}{\partial z}\right)=-\frac{\partial p}{\partial z}+2\frac{\partial}{\partial z}\left(\mu\frac{\partial w}{\partial z}\right)+\frac{\partial}{\partial y}\left(\mu\left(\frac{\partial v}{\partial z}+\frac{\partial w}{\partial y}\right)\right)+\frac{\mu}{R}\left(\frac{\partial v}{\partial z}+\frac{\partial w}{\partial y}\right). \quad (7)$$

$$\frac{\partial v}{\partial y}+\frac{v}{R}+\frac{\partial w}{\partial z}=0 \, . \quad (8)$$

Introducing the following dimensionless variables,

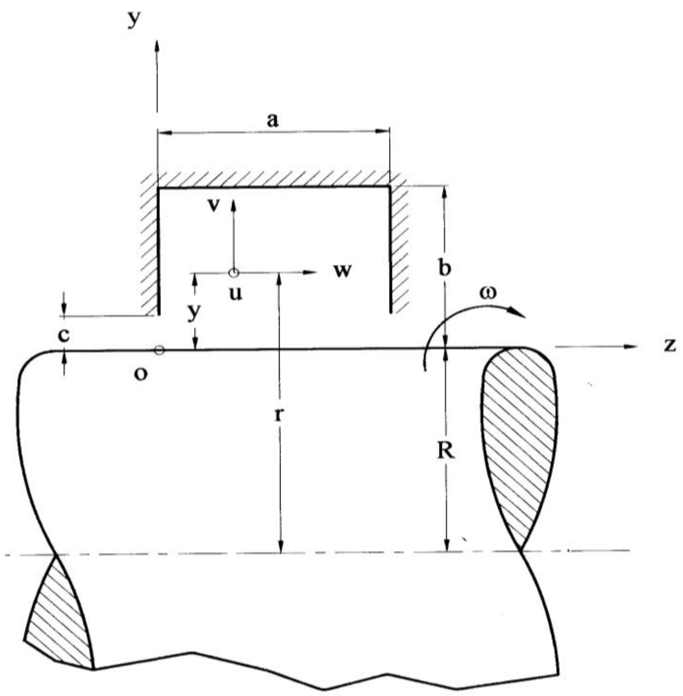

Fig. 1. Labyrinth seal geometry and coordinate system.

$$\left.\begin{aligned} &\upsilon^* = \frac{\upsilon}{U}, \; u^* = \frac{u}{U}, \; w^* = \frac{w}{U}, \; p^* = \frac{p}{\rho U^2}, \\ &y^* = \frac{y}{b}, \; z^* = \frac{z}{a} = \gamma \frac{z}{b}, \; \mu^* = \frac{\mu}{\mu_i} \\ &\text{with} \quad \gamma = \frac{b}{a}, \; m = \frac{b}{R} \text{ and } U = \frac{\mu_i}{\rho b} \end{aligned}\right\}, \tag{9}$$

Substituting from eq. (9) into eqs. (5-7 and 8) we have

$$\upsilon^* \frac{\partial \upsilon^*}{\partial y^*} + \gamma w^* \frac{\partial \upsilon^*}{\partial z^*} - m u^{*2}$$
$$= -\frac{\partial p_*}{\partial y^*} + \mu^* \left(\frac{\partial^2 \upsilon^*}{\partial y^{*2}} + \gamma^2 \frac{\partial^2 \upsilon^*}{\partial z^{*2}} + m \frac{\partial \upsilon^*}{\partial y^*} - m^2 \upsilon^* \right)$$
$$+ 2 \frac{\partial \mu^*}{\partial y^*} \frac{\partial \upsilon^*}{\partial y^*} + \gamma \frac{\partial \mu^*}{\partial z^*} \left(\gamma \frac{\partial \upsilon^*}{\partial z^*} + \frac{\partial w^*}{\partial y^*} \right), \tag{10}$$

$$\upsilon^* \frac{\partial u^*}{\partial y^*} + \gamma w^* \frac{\partial u^*}{\partial z^*} + m u^* \upsilon^* = \gamma^2 \frac{\partial}{\partial z^*} \left(\mu^* \frac{\partial u^*}{\partial z^*} \right)$$
$$+ \frac{\partial}{\partial y^*} \left(\mu^* \left(\frac{\partial u^*}{\partial y^*} - m u^* \right) \right)$$
$$+ 2 \mu^* m \left(\frac{\partial u^*}{\partial y^*} - m u^* \right), \tag{11}$$

$$\upsilon^* \frac{\partial w^*}{\partial y^*} + \gamma w^* \frac{\partial w^*}{\partial z^*} = -\gamma \frac{\partial p^*}{\partial z^*}$$
$$+ 2\gamma^2 \frac{\partial}{\partial z^*} \left(\mu^* \frac{\partial w^*}{\partial z^*} \right) + \frac{\partial}{\partial y^*} \left(\mu^* \left(\gamma \frac{\partial \upsilon^*}{\partial z^*} + \frac{\partial w^*}{\partial y^*} \right) \right)$$
$$+ m \left(\gamma \frac{\partial \upsilon^*}{\partial z^*} + \frac{\partial w^*}{\partial y^*} \right). \tag{12}$$

$$\frac{\partial \upsilon^*}{\partial y^*} + m \upsilon^* + \gamma \frac{\partial w^*}{\partial z^*} = 0. \tag{13}$$

Assuming $m << 1$ and introducing the following series expansions in power of *m*:

$$\left.\begin{aligned} u^* &= u_o + m u_1 + m^2 u_2 + \cdots \\ v^* &= \quad m v_1 + m^2 v_2 + \cdots \\ w^* &= \quad m w_1 + m^2 w_2 + \cdots \\ p^* &= \quad m p_1 + m^2 p_2 + \cdots \\ \mu^* &= \mu_o + m \mu_1 + m^2 \mu_2 + \cdots \end{aligned}\right\}. \tag{14}$$

Substituting from eqs. (14 into 11) and retaining terms of order m^0 we get,

$$0 = \gamma^2 \frac{\partial}{\partial z^*}\left(\mu_o \frac{\partial u_o}{\partial z^*}\right) + \frac{\partial}{\partial y^*}\left(\mu_o \frac{\partial u_o}{\partial y^*}\right). \tag{15}$$

Substituting from eqs. (14 into 10, 12 and 13) and retaining terms of order m^1 we get,

$$-u_o^{*2} = -\frac{\partial p_1}{\partial y^*} + \mu_o\left(\frac{\partial^2 v_1}{\partial y^{*2}} + \gamma^2 \frac{\partial^2 v_1}{\partial z^{*2}}\right) + 2\frac{\partial \mu_o}{\partial y^*}\frac{\partial v_1}{\partial y^*} + \gamma \frac{\partial \mu_o}{\partial z^*}\left(\gamma \frac{\partial v_1}{\partial z^*} + \frac{\partial w_1}{\partial y^*}\right). \tag{16}$$

$$0 = -\gamma \frac{\partial p_1}{\partial z^*} + 2\gamma^2 \frac{\partial}{\partial z^*}\left(\mu_o \frac{\partial w_1}{\partial z^*}\right) + \frac{\partial}{\partial y^*}\left(\mu_o\left(\gamma \frac{\partial v_1}{\partial z^*} + \frac{\partial w_1}{\partial y^*}\right)\right), \tag{17}$$

and

$$\frac{\partial v_1}{\partial y^*} + \gamma \frac{\partial w_1}{\partial z^*} = 0. \tag{18}$$

Rearranging eqs. (15-17) and using eq. (18) we have,

$$0 = \mu_o\left(\frac{\partial^2 u_o}{\partial y^{*2}} + \gamma^2 \frac{\partial^2 u_o}{\partial z^{*2}}\right) + \frac{\partial \mu_o}{\partial y^*}\frac{\partial u_o}{\partial y^*} + \gamma^2 \frac{\partial \mu_o}{\partial z^*}\frac{\partial u_o}{\partial z^*}, \tag{19}$$

$$-u_o^2 = -\frac{\partial p_1}{\partial y^*} + \mu_o\left(\frac{\partial^2 v_1}{\partial y^{*2}} + \gamma^2 \frac{\partial^2 v_1}{\partial z^{*2}}\right) + \frac{\partial \mu_o}{\partial z^*}\left(\frac{\partial v_1}{\partial y^*} - \gamma \frac{\partial w_1}{\partial z^*}\right) + \gamma \frac{\partial u_o}{\partial z^*}\left(\gamma \frac{\partial v_1}{\partial z^*} + \frac{\partial w_1}{\partial y^*}\right). \tag{20}$$

$$0 = -\gamma \frac{\partial p_1}{\partial z^*} + \mu_o\left(\frac{\partial^2 w_1}{\partial y^{*2}} + \gamma^2 \frac{\partial^2 w_1}{\partial z^{*2}}\right) + \gamma^2 \frac{\partial \mu_o}{\partial z^*}\frac{\partial w_1}{\partial z^*} + \frac{\partial \mu_o}{\partial y^*}\left(\gamma \frac{\partial v_1}{\partial z^*} + \frac{\partial w_1}{\partial y^*}\right). \tag{21}$$

It is seen that the zeroth order eq. (19) is uncoupled from the system of first order eqs. (18, 20 and 21).

The energy equation for the flow in the seal may be written as,

$$\rho C_p\left(v\frac{\partial T}{\partial y} + w\frac{\partial T}{\partial z}\right) = K\left(\frac{\partial^2 T}{\partial y^2} + \frac{1}{R}\frac{\partial T}{\partial y} + \frac{\partial^2 T}{\partial z^2}\right) + \phi), \tag{22}$$

with

$$\phi = \mu\left[\begin{aligned} &2\left\{\left(\frac{\partial v}{\partial y}\right)^2 + \frac{v^2}{R_2} + \left(\frac{\partial w}{\partial z}\right)^2\right\} \\ &+\left(\frac{\partial u}{\partial z}\right)^2 + \left(\frac{\partial v}{\partial y} + \frac{\partial w}{\partial y}\right)^2 + \left(\frac{\partial u}{\partial y} - \frac{u}{R}\right)^2 \end{aligned}\right]. \tag{23}$$

Eq. (22) may be written in dimensionless form as,

$$v^* \frac{\partial T^*}{\partial y^*} + \gamma w^* \frac{\partial T^*}{\partial z^*} = \frac{1}{P}\left(\frac{\partial^2 T^*}{\partial y^{*2}} + m\frac{\partial T^*}{\partial y^*} + \gamma^2 \frac{\partial^2 T^*}{\partial z^{*2}}\right) + E\phi^*, \tag{24}$$

with

$$\phi^* = \mu^*\left[\begin{aligned} &2\left\{\left(\frac{\partial v^*}{\partial y^*}\right)^2 + m^2 v^{*2} + \gamma^2\left(\frac{\partial w^*}{\partial z^*}\right)^2\right\} \\ &+\gamma^2\left(\frac{\partial u^*}{\partial z^*}\right)^2 + \left(\gamma \frac{\partial v^*}{\partial z^*} + \frac{\partial w^*}{\partial y^*}\right)^2 \\ &+\left(\frac{\partial u^*}{\partial y^*} - m u^*\right)^2 \end{aligned}\right], \tag{25}$$

where $P = \frac{\mu_i C_p}{K}$, $E = \frac{U^2}{C_p T_i} = \frac{\mu_i^2}{\rho^2 b^2 C_p T_i}$ are the Prandtl number and Eckert number respectively, and $T^* = T/T_i$.

Assuming the following series expansion for the dimensionless temperature T^*:

$$T^* = T_o + m T_1 + m^2 T_2 + \cdots . \tag{26}$$

Substituting from eq. (26) into eq. (24 and 25 and retaining terms of order m^0 only we have,

$$\frac{\partial^2 T_o}{\partial y^{*2}} + \gamma^2 \frac{\partial^2 T_o}{\partial z^{*2}} = -\Lambda \mu_o \left[\left(\frac{\partial u_o}{\partial y^*} \right)^2 + \gamma^2 \left(\frac{\partial u_o}{\partial z^*} \right)^2 \right], \tag{27}$$

where

$$\Lambda = E P = \frac{\mu_i^3}{\rho^2 K b^2 T_i} \cdot$$

For the purpose of modeling the temperature dependence on the fluid rheology, the viscosity is modeled with the exponential type of dependence as:

$$\mu = \mu_i \, e^{-\beta (T_i - T)}, \tag{28}$$

and in dimensionless form as,

$$\mu^* = e^{-\beta^* \left(1 - T^*\right)}. \tag{29}$$

Substituting from eq. (14 and 16) into 29) and retaining terms of order m^0 we get,

$$\mu_o = e^{-\beta^* (1 - T_o)}. \tag{30}$$

Eqs. (19 and 27) may be rewritten as,

$$\frac{\partial^2 u_o}{\partial y^{*2}} + \gamma^2 \frac{\partial^2 u_o}{\partial z^{*2}} - \left(\beta^* \frac{\partial T_o}{\partial y^*} \right) \frac{\partial u_o}{\partial y^*} - \left(\beta^* \gamma^2 \frac{\partial T_o}{\partial z^*} \right) \frac{\partial u_o}{\partial z^*} = 0 . \tag{31}$$

$$\frac{\partial^2 T_o}{\partial y^{*2}} + \gamma^2 \frac{\partial^2 T_o}{\partial z^{*2}} + \Lambda e^{-\beta^* (T_o - 1)} \left[\left(\frac{\partial u_o}{\partial y^*} \right)^2 + \gamma^2 \left(\frac{\partial u_o}{\partial z^*} \right)^2 \right] = 0 . \tag{32}$$

Eqs. (31 and 32) are subject to the following boundary conditions:

$$\left.\begin{array}{llll}
At & y^* = 0 , & u_o = \lambda = \dfrac{\rho \omega R b}{\mu_i} , & \dfrac{\partial T_o}{\partial y^*} = 0 \\
At & y^* = 1 , & u_o = 0 , & \dfrac{\partial T_o}{\partial y^*} = 0 \\
At & z^* = 0 \text{ or } 1 \text{ and } c^* \le y^* \le 1 , & u_o = 0 , & \dfrac{\partial T_o}{\partial z^*} = 0 \\
At & z^* = 0 \quad \text{and } 0 \le y^* \le c^* , & \dfrac{\partial u_o}{\partial z^*} = 0 , & T_o = 1 \\
At & z^* = 1 \quad \text{and } 0 \le y^* \le c^* , & \dfrac{\partial u_o}{\partial z^*} = 0 , & T_o = \left(1 - \dfrac{\Delta T_i}{T_i} \right)
\end{array}\right\} . \tag{33}$$

The governing eqs. (31 and 32) along with their boundary conditions (33) can be solved numerically using the finite difference technique and SOR method [10]. A step size of 0.05 in y^* and z^* is used and found suitable for numerical computations.

3. Results and discussion

Figs. 2-a, b, c and d show the variation of the dimensionless heat flow at inlet clearance

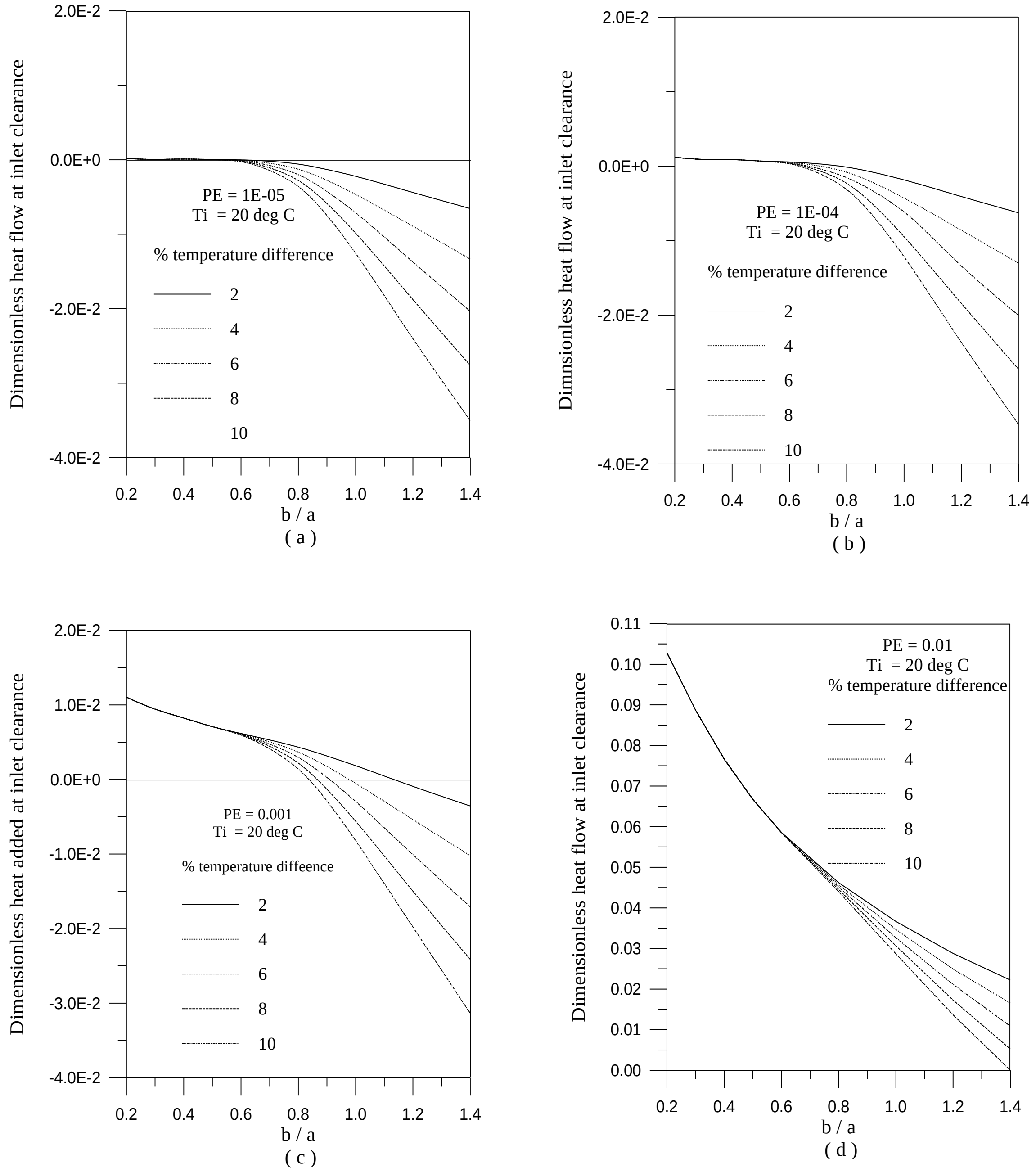

(a) $P.E = 1E-05$ (b) $P.E = 1E-05$

(c) $P.E = 1E-05$ (d) $P.E = 1E-05$

Fig. 2. The variation of heat flow at inlet clearance with seal aspect ratio for different values of $P.E$ and percentage temperature difference.

$\left.\frac{\partial T_o}{\partial z^*}\right|_{\substack{z^*=0\\0\le y^*\le c^*}}$ with the seal aspect ratio, $\gamma = b/a$.

For a given temperature difference between inlet and exit clearances $(T_i - T_e) > 0$, this variation is affected considerably by the product of Prandtl number and Eckert number P.E. At small values of P.E the heat is added at inlet clearance as long as the aspect ratio is approximately less than 0.6. The amount of this added heat increases with the increase in P.E for a given value of the temperature difference. Increasing the aspect ratio decreases the amount of heat added and this becomes more pronounced as P.E increases. Fig. 3 is a reproduction of figs. 2 for a specific value of aspect ratio, γ = 1. It can be seen clearly that for the whole range of percentage temperature difference heat can be rejected if P.E is smaller than approximately 0.0025 depending on the value of the percentage temperature difference. It is noted that for a given value of the temperature difference heat is added to the fluid at inlet clearance as long as the aspect ratio does not exceed a certain value defined here as the critical aspect ratio, γ_{cr}. A reversal of the direction of the flow of heat at the inlet clearance occurs when the temperature gradient at it changes sign. This effect is of fundamental importance for the consideration of heat loss through sealing process. Fig.4 shows that the selection of the aspect ratio depends on the temperature difference and P.E. It can be seen that for a certain value of P.E and at a specified temperature difference, if $\gamma < \gamma_{cr}$, the heat is added at inlet clearance. For a given temperature difference between the inlet and exit clearances $(\Delta T^* = 10\%)$, Figs. 5-a and b show the effect of P.E on the dimensionless fluid velocity u^* along the seal cavity in the plane of symmetry $z^* = 0.5$ for aspect ratio γ = 1. The isothermal solution is also plotted in the figures. The small value of P.E has a small effect on the fluid velocity, fig. 5a. Increasing P.E decreases the velocity especially close to the stationary wall, fig. 5b. Also, at the same temperature difference and aspect ratio, figs. 6a and b show the variation of the dimensionless fluid temperature along the seal cavity in the plane of symmetry. Increasing P.E increases the fluid temperature over the value of the wormer inlet clearance temperature. This effect becomes more pronounced close to the rotating wall. At (ΔT^* = 10%), P.E =1 and γ = 1, fig. 7 shows the isotherms inside the seal cavity. The generation of heat due to friction exerts a large effect on the process of heat flow and that at large value of P.E the wormer clearance may become heated instead of being cooled.

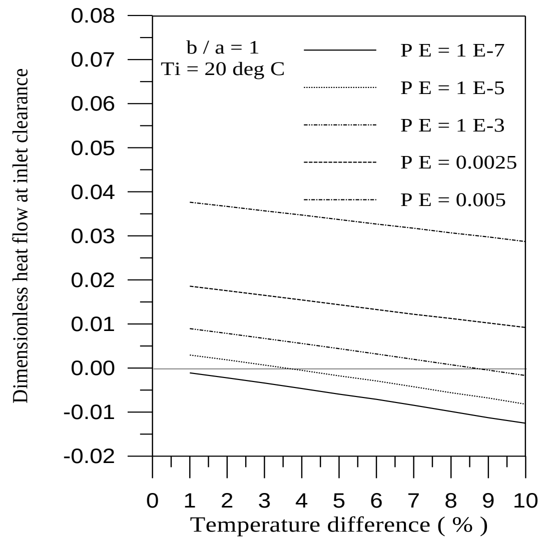

Fig. 3. Effect of P.E on the variation of heat flow at inlet clearance with percentage temperature difference.

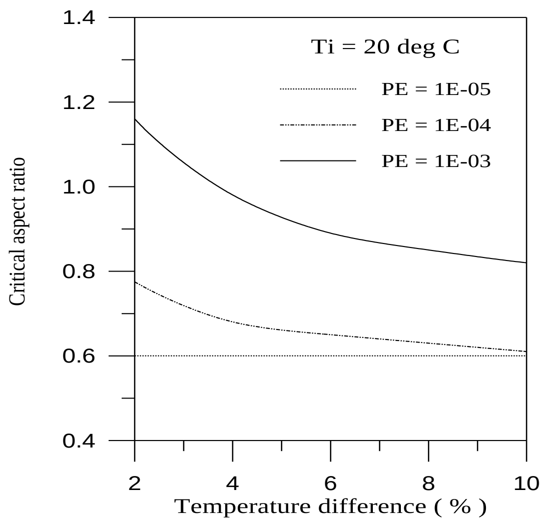

Fig. 4. The variation of the critical aspect ratio with percentage temperature difference for different values of product P.E.

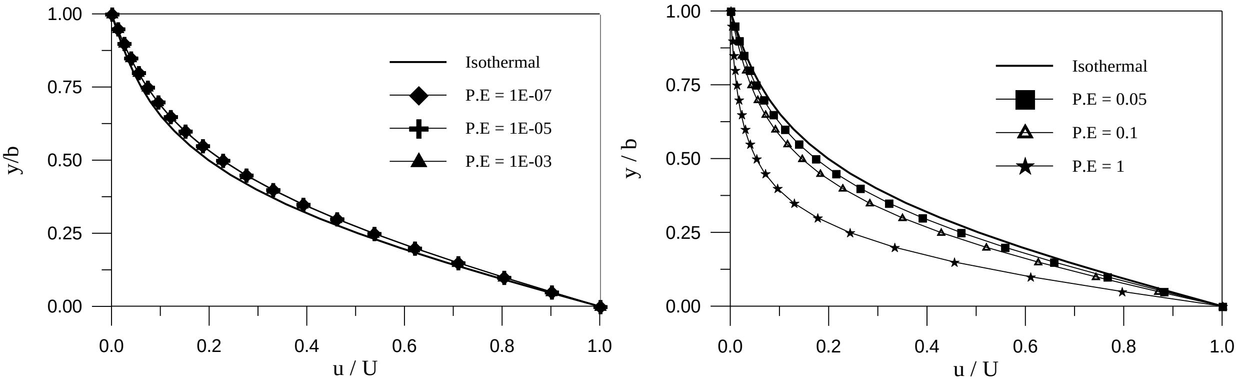

(a) Case of heat rejection at inlet clearance (b) Case of heat added at inlet clearance

Fig. 5. The velocity along the seal cavity in the plane of symmetry for γ= 1 and ΔT^* = 10% at different values of P.E.

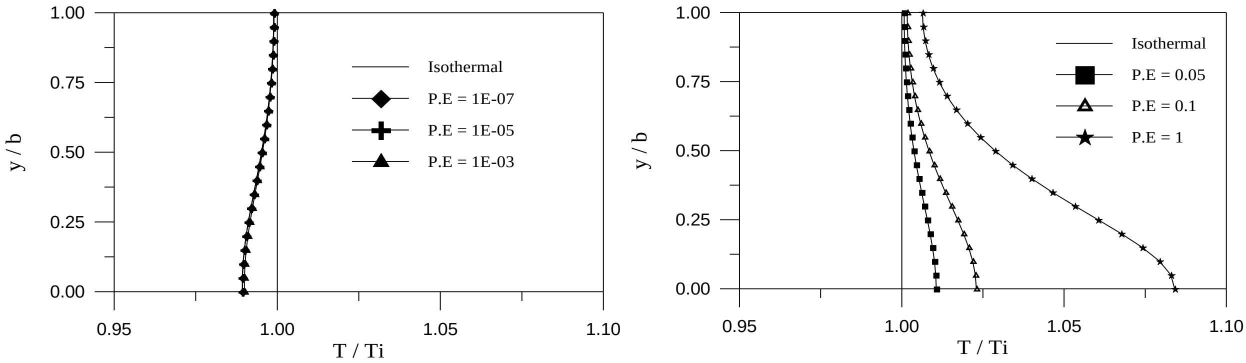

(a) Case of heat rejected at inlet clearance (b) Case of heat added at inlet clearance

Fig. 6. The temperature distribution along the seal cavity in the plane of symmetry for γ= 1 and ΔT^* = 10% at different values of P.E.

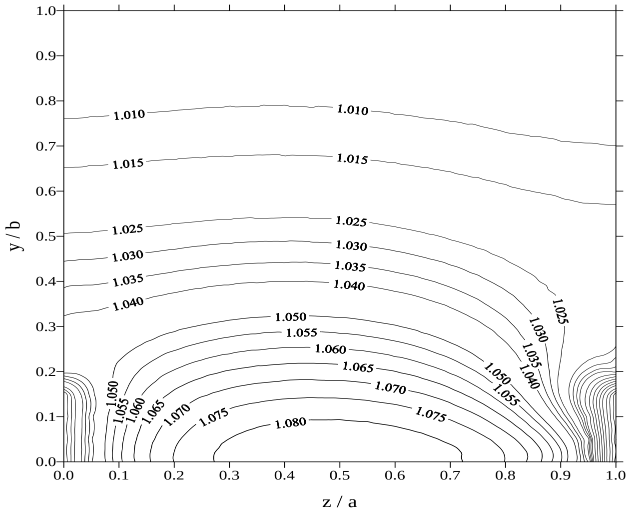

Fig. 7. Isotherms inside the seal cavity at 10% temperature difference between inlet and exit clearances for γ= 1 and P.E =1.

4. Conclusions

1. The variation of heat flow at inlet clearance is affected considerably by the product of Prandtl number and Eckert number P.E.
2. At small values of P.E the heat is rejected at inlet clearance as long as the aspect ratio is approximately less than 0.6.
3. For a given aspect ratio, increasing P.E increases the generation of heat due to friction and the wormer clearance may become heated instead of being cooled.
4. The aspect ratio defined here as the critical aspect ratio depends on the temperature difference between the inlet and exit clearances and P.E.

Nomenclature

a	is the labyrinth width, m,
b	is the labyrinth height, m,
c	is the labyrinth clearance, m,
c^*	is the dimensionless labyrinth clearance, $c^* = c/b$,
C_p	is the fluid specific heat at constant pressure, $J/kg\,K$,
E	is the eckert number, $E = \mu_i^2 / \rho^2 b^2 g c_p T_i$,
g	is the gravitational acceleration, m/s^2,
K	is the fluid thermal conductivity, $W/m\,K$,
m	is the labyrinth height to shaft radius ratio, $m = b/R$,
p	is the fluid pressure, Pa,
p^*	is the dimensionless fluid pressure, $p^* = p/\rho U^2$,
P	is the Prandtl number, $P = \mu_i g c_p / K$,
m	is the radial distance, m,
R	is the Shaft radius, m,
T	is the fluid temperature, *K*,
T^*	is the Dimensionless fluid temperature, $T^* = T/T_i$,
ΔT_i	is the temperature difference across the seal cavity, *K*,
U	is the characteristic velocity, $U = \mu_i / \rho b$, m/s,
u, v, w	are the velocity components in tangential, radial and axial directions respectively, m/s,
u^*, v^*, w^*	are the dimensionless velocity components, $u^* = u/U$, $v^* = v/U$, $w^* = w/U$,
Y	is the radial transformed coordinate, m,
y^*	is the dimensionless transformed coordinate, $y^* = y/b$,
z	is the axial coordinate distance, m,
z^*	is the dimensionless axial coordinate, $z^* = z/a$,
β	is the viscosity temperature index, K^{-1},
β^*	is the dimensionless viscosity index, $\beta^* = \beta T_i$,
γ	is the aspect ratio, $\gamma = b/a$,
λ	is the rotation parameter, $\lambda = \rho \omega R b / \mu_i$,
Λ	is the dissipation number, $\Lambda = E P = \mu_i^3 / \rho^2 K b^2 T_i$,
μ	is the fluid viscosity, Pa s,
μ_i	is the fluid viscosity at inlet, Pa s,
μ^*	is the dimensionless fluid viscosity, $\mu^* = \mu/\mu_i$,
ρ	is the fluid density, kg/m^3, and
ω	is the shaft angular velocity, rad/s.

References

[1] E. Benvenuti, G. Ruggrei and E.P. Tomasini, "Analytical and Experimental Development of Labyrinth Seals for Process Centrifugal Compressors", ASME, NY, pp. 287-285 (1979).

[2] H. Stoff, "Incompressible Flow in a Labyrinth Seal", J. Fluid Mech., Vol. 100 (4), pp. 817-829 (1981).

[3] D.L. Rhode, J.A. Demko, V.K. Tracgner Morison and C.L. Sobobick, "Prediction of the Incompressible Flow in Labyrinth Seals", J. of Fluids Engineering for Gas

Turbines and Power, Vol. 108, pp. 19-25 (1986).
[4] D.L. Rhode and S.R. Sobolich, "Simulation of Subsonic Flow Through a Generic Labyrinth Seal", J. of Fluids Engineering for Gas Turbines and Power, Vol. 108, pp. 674-680 (1986).
[5] H.A. El-Gamal T.H. Awad and E.E. Saber, "Effect of Lateral Misalignment on the Performance and Dynamic Characteristics of Labyrinth Seals", The 8th Inter. Conference for Mech. Power Eng. Alexandria Univ. Apr. 27-29, pp. 159-177 (1993).
[6] H.A. El-Gamal, T.H. Awad and E.E. Saber, "Leakage From Labyrinth Seals Under Stationary and Rotating Conditions", Tribology Inter., Vol. 29, pp. 291-297 (1996).
[7] E. Saber, "A Model for a Labyrinth Seal of Arbitrary Shape", AEJ (2002).
[8] K. Kwanka, "Dynamic Coefficients of Stepped Labyrinth Gas Seals", Journal of Engineering for Gas Turbine and Power, Vol. 122, pp. 473-477 (2000).
[9] J.J. Moor, "Three Dimensional CFD Rotodynamic Analysis of Gas Labyrinth Seals", Journal of Vibration and Acoustics, Vol. 125, pp. 427-433 (2003).
[10] G.D. Smith, "Numerical Solution of Partial Differential Equations", Oxford Univ. Press, Oxford (1971).

Received July 30, 2007
Accepted January 29, 2008